

1 1. Title: Characterisation of elastic and acoustic properties of an agar-based tissue  
2 mimicking material.

3 Authors:

- 4 1. M.P.Brewin, Blizard Institute, Barts and The London School of Medicine and Dentistry,  
5 Queen Mary University of London, London, UK
- 6 2. M.J.Birch, Clinical Physics, Barts Health NHS Trust, 56-76 Ashfield Street, London, UK
- 7 3. D.J.Mehta, Blizard Institute, Barts and The London School of Medicine and Dentistry,  
8 Queen Mary University of London, London, UK
- 9 4. J.W.Reeves, Clinical Physics, Barts Health NHS Trust, 56-76 Ashfield Street, London,  
10 UK
- 11 5. S.Shaw, BICOM (Brunel Institute of Computational Mathematics) and Mathematics,  
12 Brunel University, UK
- 13 6. C. Kruse, BICOM (Brunel Institute of Computational Mathematics) and Mathematics,  
14 Brunel University, UK
- 15 7. J.R. Whiteman, BICOM (Brunel Institute of Computational Mathematics) and  
16 Mathematics, Brunel University, UK
- 17 8. S.Hu, Center for Research in Scientific Computation, North Carolina State University,  
18 Raleigh, NC, USA
- 19 9. Z.R.Kenz, Center for Research in Scientific Computation, North Carolina State  
20 University, Raleigh, NC, USA
- 21 10. H.T.Banks, Center for Research in Scientific Computation, North Carolina State  
22 University, Raleigh, NC, USA

1 11. S.E. Greenwald, Blizard Institute, Barts and The London School of Medicine and  
2 Dentistry, Queen Mary University of London, London, UK

3

4 Running Head: Acoustic and elastic properties of an agar tissue mimic

5

6 Corresponding Author: S.E. Greenwald, Blizard Institute, Barts and the London School of  
7 Medicine and Dentistry, Queen Mary University of London, UK

8 Telephone: +44 (0) 20 3246 0178

9 Fax: +44 (0) 20 3246 0216

10 Email: [s.e.greenwald@qmul.ac.uk](mailto:s.e.greenwald@qmul.ac.uk)

## 1 2. Abstract

2 As a first step towards an acoustic localisation device for coronary stenosis to provide a non-  
3 invasive means of diagnosing arterial disease, measurements are reported for an agar-based  
4 tissue mimicking material of the propagation velocity, attenuation and viscoelastic constants,  
5 together with one dimensional quasi-static elastic moduli and Poisson's ratio. Phase speed and  
6 attenuation coefficients, determined by generating and detecting shear waves piezo-electrically  
7 in the range 300 Hz - 2 kHz, were  $3.2 - 7.5 \text{ ms}^{-1}$  and  $320 \text{ dB m}^{-1}$ . Quasi-static Young's modulus,  
8 shear modulus and Poisson's ratio, obtained by compressive or shear loading of cylindrical  
9 specimens were 150 - 160 kPa; 54 - 56 kPa and 0.37 - 0.44. The dynamic Young's and shear  
10 moduli, derived from fitting viscoelastic internal variables by an iterative statistical inverse  
11 solver to freely oscillating specimens were 230 kPa and 33 kPa and the corresponding relaxation  
12 times, 0.046 s and 0.036 s. The results were self-consistent, repeatable and provide baseline data  
13 required for the computational modelling of wave propagation in a phantom.

14  
15 **Keywords:** acoustic properties, acoustic localisation, coronary artery, elastic moduli, Poisson's  
16 ratio, shear modulus, shear wave, stenosis, tissue mimicking material, viscoelasticity

17

### 3. INTRODUCTION

Previous work on acoustic localisation of coronary arterial stenosis has been summarised in a review paper<sup>29</sup>. This has shown that, in principle, the detection of the shear waves generated at the vessel wall by disturbed flow may be used in the diagnosis of arterial disease. The overall aim of our research is to understand the way in which energy is transmitted from the arterial wall blood to the skin surface by simulating the propagation of these stenosis-induced shear waves, both experimentally in chest phantoms and computationally by software approximations to the underlying partial differential equations.

In this paper, our objective is to characterise the physical properties of an agar-based tissue mimicking material (TMM). Shear wave speed and attenuation were measured in the frequency range 300 to 2000 Hz as well as Young's, shear modulus modulus, and Poisson's ratio under quasi-static conditions, as well as the viscoelastic relaxation times following the sudden release of a normal or shearing load.

Water-based tissue-mimicking materials using either gelatin or agar have been investigated extensively in the ultrasonic range of frequencies to determine the acoustic properties of speed and attenuation<sup>8,23,24</sup>. They have been developed specifically as a calibrated material with acoustic properties similar to soft tissue for the purposes of both the assessment of ultrasound imaging performance and the construction of anthropomorphic phantoms<sup>25</sup>.

Our laboratory has much experience in the manufacture of tissue mimicking agarose gels as a tissue mimic<sup>5,6,30</sup>. We chose here to characterise a simplified 3% agarose gel because it is cheap

1 and easy both to manufacture and mould. Furthermore, the initial aim of our studies was for a  
2 proof of concept that shear waves, generated by a stenosis, can be transmitted through an  
3 anthropomorphic phantom of the chest constructed with this gel. Our intention is to show that  
4 shear waves generated by disturbed flow in a stenosed vessel within our chest phantom would be  
5 detectable at the surface. Further work may explore the adaptation of the TMM, or combination  
6 of TMMs, to better match the wave path in the chest.

7  
8 Recent ultrasound studies have assessed the acoustic properties of agar-based TMM<sup>7,27</sup>. The  
9 mechanical characterisation of both tissue and vessel ultrasound mimics have also been  
10 considered<sup>14,27</sup>. Dineley et al. used an Instron tensile testing machine to measure the tangent  
11 elastic modulus of polyvinyl alcohol cryogel (PVA-C) vessel mimic at strains up to 10%<sup>27</sup>.  
12 Elsewhere, hyper-frequency viscoelastic spectroscopy (HFVS) was compared to classical  
13 oscillatory rheometry to measure both the dynamic storage and loss moduli,  $G'$  and  $G''$ , of soft  
14 biomaterials<sup>21</sup>. Measurements were made on cylindrical tube samples of various mixtures of  
15 agar-gelatin at strains up to 1%.

16  
17 The results of our measurements have been used in the initial phase of the numerical simulations  
18 to establish the appropriate viscoelastic model of the TMM<sup>3,4</sup>. This TMM will then be used in  
19 the construction of a physical chest phantom.

20

## 1 4. MATERIALS AND METHODS

### 2 **Preparation of agar tissue mimicking material (TMM).**

3 Batches of TMM of approximately 0.5 litres were prepared by adding granulated, purified agar  
4 (Merck, Darmstadt, Germany) to deionised water in the ratio 3:97 by weight. Rodalon™  
5 (Benzalkonium Chloride, an antibacterial, antifungal agent) was also added to the mixture to  
6 suppress bacterial and fungal proliferation<sup>6</sup>. The mixture was stirred with a rotating coil and  
7 surface stirrer at 175 rpm and heated by a thermo-regulator (TE-10D, Techne, Stone, UK) in an  
8 insulated water bath for an hour at 96 °C. The gel was then allowed to cool slowly over a period  
9 of 2 - 3 hours to 47 °C. It was then poured into moulds where it set at approximately 43 °C. The  
10 TMM sample was removed from its moulds and its elastic properties were measured “fresh”. It  
11 was then stored in deionised water. Its weight and linear dimensions were re-measured “stored”  
12 on the following day along with its acoustic and elastic properties. All measurements were  
13 performed at room temperature ( $22 \pm 2^\circ\text{C}$ ).

14

### 15 **Elastic Properties**

#### 16 *Poisson's Ratio*

17 Height and width measurements under quasi-static conditions were made on 50 mm square  
18 TMM blocks of thickness 12.7 mm. The dimensions were measured using a travelling  
19 microscope (Griffin & George, London, UK) with a resolution of 10  $\mu\text{m}$ . The height and width  
20 of the block were first measured with no applied weight to determine its unloaded dimensions.  
21 A load of approximately 14 N was then applied to the top surface of the gel. The width and  
22 height of each side was then measured again giving the changes in these variables,  $\Delta H$  and  $\Delta W$ .  
23 Poisson's ratio ( $\nu$ ) was calculated from the two strain values as:

$$\nu = -\frac{\Delta W / W}{\Delta H / H} \quad (1)$$

where  $\Delta W/W$  is the transverse strain and  $\Delta H/H$  is the compressional strain.

#### ***Young's and Shear Modulus***

These elastic constants were determined by measuring the deformation due to the application of a known load, again under quasi-static conditions. The load was progressively increased using ten lead masses each of approximately 13 g. The experimental set-up for the measurement of each modulus is outlined in figure 1. For the Young's (compressional) modulus, the load was applied to the top of the unbound TMM cylinder via a Perspex top cap attached to the central rod. The displacement was measured using a laser displacement sensor (LDS) with 0.2  $\mu\text{m}$  resolution, (AR700, Schmitt Industries, Oregon, USA). The analogue displacement signal from the LDS was acquired in real time using a data acquisition system running LabVIEW software (version 11.0.1, National Instruments (NI), Newbury, UK). The NI system comprised an analogue input module (NI 9234) interfaced to a real-time controller (NI 9024), via a customised field-programmable gate array (NI 9116). The real-time controller digitises the signals at 17 kHz and the waveform and data are passed to a PC for display and storage. For the shear modulus, the load was applied to the inner core. This core was wrapped in abrasive paper and the TMM was moulded around it to prevent movement between the core and the TMM. Whereas the outer boundaries of the TMM cylinder were free in the compressional set up, thus allowing longitudinal movement, for the shear measurements they were fixed to the grooved Perspex cylinder into which the TMM was cast. The fixation of the boundary of the cylinder wall in this manner prevented longitudinal movement and enabled the load forces to be exerted in the shear

1 plane. The loads were applied incrementally in each set up and the gradient of the stress-strain  
2 curve was used to calculate each elastic modulus.

3  
4 For comparison, the stress-strain measurements were repeated in another laboratory (Department  
5 of Materials, Queen Mary University of London, UK) using a materials testing machine fitted  
6 with a strain gauge load cell (Instron, Norwood, MA, USA). In these experiments, the force  
7 generated by a known displacement is measured rather than the displacement resulting from a  
8 known load.

9

#### 10 *Creep*

11 Viscoelastic creep was also investigated using both the compressional and shear set up on TMM  
12 cylinders shown in Figure 1. A load of 48.0 g was applied. The measurement set up was housed  
13 in a temperature controlled water bath to minimise the effect of room temperature changes  
14 which, in preliminary experiments, had been shown to cause displacements comparable to those  
15 resulting from the applied load. The water also prevented dehydration of the gel. A thermo-  
16 regulator (Techne TE10D, Bibby Scientific, Stone, UK) maintained the water bath temperature  
17 at  $24.9 \pm 0.2^\circ\text{C}$  for the duration of the study. A miniature thermocouple (K-type, Omega, UK)  
18 was embedded in the gel. The temperature of the gel was recorded using the National  
19 Instruments data capture hardware and LabVIEW software at a sampling rate of 0.1 Hz. The gel  
20 was allowed to equilibrate in the water bath for approximately 2 hours before the 48.0 g load was  
21 applied.

1  
2  
3  
4  
5  
6  
7  
8  
9  
10  
11  
12  
13  
14  
15  
16  
17  
18  
19  
20  
21  
22  
23

***Free Oscillations***

In order to investigate further the viscoelastic behaviour of the TMM and provide a diverse range of data for the mathematical modelling of its properties, free oscillations were induced within the cylinder in both the compressional and shear set-ups. One of four different loads, 66 g, 132 g, 198 g and 264 g, was applied to the central rod via a nylon filament having a diameter of 0.35 mm. After a few seconds, while the load on the end of the filament was allowed to stabilise, it was then rapidly released, over a time period of 10 ms, by burning through the filament with a blow torch flame. Time-displacement curves for each load and set-up were captured using the LabVIEW software.

**Shear Wave Acoustic Properties**

The acoustic measurements were carried out only on samples that had been stored in water overnight. In order to make the measurements using the substitution technique, as described below, an acoustic transmitter and receiver were used. The transmitting accelerometer (TR0APN, PCB Piezotronics, Depew, NY, US), that is shown as  $T_x$  in figure 2, was manufactured as a receiver. However, here, it acted as a shear wave transmitter by application of a drive voltage to the output terminals. The driving frequency of the transmitter was set on the function generator and the amplified driving voltage was 141 V. A tone-burst of 40 cycles was used for the measurements. The drive was produced by a 700 Watt audio amplifier (SX-2800, Samson, Hauppauge, NY, US) being itself driven by a function generator (33250A, Agilent, Santa Clara, CA, US). A digital oscilloscope (LT264, LeCroy, Chestnut Ridge, NY, US) allowed the input and output signal to and from the amplifier to be viewed in real time. A shear

1 stress was created by the induced vibration and consequent strain propagated as a wave in the  
2 tissue mimicking material.

3  
4 The shear waves were detected at the opposite face of the TMM by an accelerometer (Y352A24,  
5 PCB Piezotronics, Depew, NY, US), shown as  $R_x$  in figure 2, with physical dimensions of 12 x 7  
6 x 4 mm and weighing 0.8 g. This is responsive only to displacements in a single plane defined  
7 parallel to the base, or surface, of the device. This receiver was connected to the analogue input  
8 module (NI9234), which is configured for IEP-type transducers, by a low-noise Teflon cable.  
9 The transmit, receive and synchronisation signals were passed from the controller by Ethernet  
10 connection to the PC. This enabled the modulus and phase of the received signal power  
11 spectrum, derived from a fast Fourier transform, to be displayed in real time. The PC provided  
12 control of the real time acquisition parameters, phase of the transmitted and received shear  
13 waves, extended real time measurements for the longer duration TMM creep measurements and  
14 enabled data storage and output as text files for further analysis.

15

### 16 ***Attenuation***

17 Attenuation was measured using the insertion or substitution technique <sup>1,5</sup>. By comparison of the  
18 signal strength received through different path lengths, the attenuation per unit distance at  
19 various frequencies can be obtained. The transmit signal was injected at fixed frequencies from  
20 300 to 2500 Hz at increments of 100 Hz. The relative signal strength in dB of transmitted  
21 signals at the receiver was assessed as the amplitude at the peak frequency of the power  
22 spectrum. The signal amplitude in dB was then calculated for different block thicknesses  
23 normalised to the thinnest specimen. The thicknesses of the 50 mm square specimen blocks

1 were 15, 30, 45 and 60 mm. The  $V_{\text{rms}}$  signal was acquired from the  $R_x$  accelerometer voltage  
2 output, calibrated from manufacturer's data to give shear wave acceleration in units of  $\text{ms}^{-2}$ . The  
3 peak amplitude of each power spectrum was measured, using an electronic cursor on the  
4 LabVIEW screen, ten times per TMM block. The data were averaged and the attenuation in dB  
5  $\text{cm}^{-1}$  was calculated using the expression:

$$6 \quad A(f, x, y) = \frac{(P_1(f, x, y) - P_0(f, x, y))}{d} \quad (2)$$

7 where  $P_1$  and  $P_0$  are the average peak power spectral amplitudes of the signal through two  
8 different TMM blocks in dB, and  $d$  is the difference in path length travelled by each signal, i.e.  
9 the difference in thickness between any two blocks.

10

### 11 *Velocity*

12 The velocity of the shear waves in the TMM was derived from the transit time of the wave along  
13 a known path length. The transit time was found by measurement of the phase difference  
14 between transmission and reception of the shear wave. In this experiment, the phase difference  
15 between transmit and receive signals was measured at frequencies between 300 and 2000 Hz, at  
16 100 Hz intervals. The phase difference was expressed as a time shift ( $\Delta t$ ) in the signal, as shown  
17 in equation 3, for a known change in beam path length, which is equivalent to the difference in  
18 TMM thickness.

$$19 \quad \Delta t(f) = \frac{\phi_1(f) - \phi_0(f)}{2\pi f} \quad (3)$$

20 where  $\phi_1$  and  $\phi_0$  are the phase in radians for different thicknesses and  $f$  is the frequency.

1 The phase change was adjusted by  $2n\pi$  radians as necessary in order to account for any phase  
2 change greater than one wavelength or time period. The jumps in  $2\pi$  are apparent from the plot  
3 of phase change against frequency. The phase velocity was then calculated knowing the  
4 difference in TMM thickness between the blocks.

5

## 6 **5. RESULTS**

7 The Poisson's ratio for fresh TMM was  $0.37 \pm 0.07$  (SD,  $n = 3$ ) and for that stored in water was  
8  $0.44 \pm 0.08$  ( $n = 7$ ), where  $n$  is the number of samples measured. Young's modulus measured  
9 when axially compressing the sample was in the range of  $110 - 120 \pm 4$  kPa (mean  $\pm$  SD) for  
10 fresh TMM and in the range  $150 - 160 \pm 8$  kPa after storage in water. The values for shear  
11 modulus were  $53 \pm 2$  kPa for fresh TMM and  $55 \pm 2$  kPa for stored TMM. These data are  
12 compared with the values measured for the moduli using the incremental load (LDS) and Instron  
13 methods, as shown in table 1, which also allows comparison between the shear modulus values  
14 measured by the LDS and Instron methods.

15

16 The creep curve is shown for both the compressional and shear set up in figures 3 & 4. The  
17 unloaded displacement was set to zero and the displacement is normalised to the initial loaded  
18 displacement. It became apparent that, with the load applied for nearly 30 hours for the shear  
19 and 50 hours for the compression measurements, the creep on the gels did not show signs of  
20 stopping. The load was then released and the gel was allowed to settle. For the axial creep  
21 under compression, shown in figure 3, it is apparent that the load of Perspex lid and rod caused a  
22 continued creep of the gel following the removal of the applied load at the 50 hour mark. For the  
23 shear creep, shown in figure 4, the gel tends towards its original displacement for 30 hours

1 before the extant load causes the gel to creep again. Note that the initial displacement of the gel  
2 when subjected to the axial load is approximately 6 times greater than when it is sheared with a  
3 similar load, the differing y-axis scales accounting for the apparently greater noise in the shear  
4 experiment. The stresses due to the 48 g load were 189 and 253 N m<sup>-2</sup> for the axial and shear  
5 cases, respectively. Allowing for the greater stress in the shear experiment (shear to axial stress  
6 ratio 4:3 and the difference between the shear and Young's modulus values, ratio 3:1), the  
7 expected initial strain ratio would be approximately 4:1, which is inconsistent with the observed  
8 ratio of 6:1.

9  
10 The free oscillations following abrupt unloading of the TMM for the compressional and shear set  
11 ups are shown in figures 5 & 6. These representative plots are for the 264 g load. The other  
12 loads produced similar qualitative behaviour (number of repeats, n = 9 for each load). The top  
13 section of each figure panel shows the entire time course of the experiment for the fresh and  
14 stored cylinders. The system is at rest before the load is added at t = 1 to 2 seconds. The load is  
15 then released at t = 3.5 s (compressional) and at t = 4.2 s (shear). The oscillations occur as the  
16 system returns towards equilibrium. The lower panels of each figure show the oscillations at an  
17 expanded time scale. The gel specimens in both the shear and the compressional set-ups  
18 oscillated at frequencies between 50 and 60 Hz. The dynamic Young's modulus and relaxation  
19 time for a representative stored specimen subjected to a load of 264 g were 230 kPa and 0.046 s.  
20 The corresponding values for the shear experiment were 33.4 kPa and 0.036 s. More details of  
21 the fitting procedure and error analysis can be found in a companion paper<sup>3</sup>.

22

1 The acoustic property measurements were repeated six times for both attenuation and velocity.  
2 The values of attenuation are normalised to the 15 mm thick block and are plotted against  
3 frequency in the range 300 - 2500 Hz as shown in figure 7. A straight line is fitted to the data  
4 from the 60mm specimen. There was a highly significant correlation between frequency and  
5 attenuation, ( $r^2 = 0.65$ ,  $P < 0.001$ ), although it is clear that there are regular fluctuations either  
6 side of the line, with an approximate period of 400 Hz. The shear phase speed was calculated for  
7 each block thickness over the frequency range 300 - 2000 Hz. The frequency dependence of  
8 phase speed is plotted in figure 8. The average value over the thicknesses is shown by the dark  
9 line. The range of shear phase speed is  $3.2 - 7.5 \text{ ms}^{-1}$ .

10

## 11 **6. DISCUSSION**

### 12 **Elastic Properties**

13 As the TMM must be kept hydrated to avoid changes in physical properties due to dehydration, it  
14 was deemed necessary to characterise any change in its properties following storage in water.  
15 The proposed anthropomorphic phantoms will be kept in water as they may need to be tested  
16 over many hours and perhaps days. The reason for this change in properties remains to be  
17 understood and could form the basis of further studies.

18

19 Measured values of Poisson's ratio in the fresh TMM were significantly lower than those in the  
20 stored specimens ( $0.37 \pm 0.07$  ( $n = 3$ ) and  $0.44 \pm 0.08$  ( $n = 7$ ) respectively,  $\pm 1$  SD), both values  
21 being less than the majority quoted in the literature. Indeed, many studies assume the material is  
22 incompressible and therefore quote an assumed value of  $\sim 0.5$ <sup>19,26</sup>. We note in passing that the  
23 95% confidence interval of the stored specimen encompasses values greater than 0.5, which

1 reflects the variability in the measurements rather than the reality of values greater than 0.5. One  
2 study measured both elastic modulus and Poisson's ratio of a 3 % agar gel and obtained a value  
3 for Poisson's ratio of 0.32<sup>28</sup>. Similar blood vessel mimicking materials such as PVA cryogel  
4 have also been measured with a Poisson's ratio in the range of 0.42 - 0.48<sup>16</sup>. Our TMM has  
5 similar values to that of lead at  $\sim 0.44$  and copper at  $\sim 0.34 - 0.37$ <sup>20</sup>. The measured values do  
6 not therefore seem unreasonable and we can assume that the gel is indeed compressible. To  
7 ensure that the material did not demonstrate poroelastic properties, we weighed specimens before  
8 and after subjecting them to a compressive load. For gels, typically weighing around 120g, the  
9 difference in weight between pre- and post-loading was less than 0.5g and in some cases was not  
10 detectable. We assume that the compressibility of the gel is not due to the exudation of water  
11 when subjected to a compressive load.

12  
13 However, our measured values for Poisson's ratio, Young's modulus and shear modulus are  
14 internally consistent. To our knowledge, this has not been shown before in agar gels. By  
15 application of the Lamé expression<sup>15</sup>,  $E = 2G(1+\nu)$ , where  $G$  is the shear modulus and  $\nu$ ,  
16 Poisson's ratio, we find that these values along with our results for Young's and shear Modulus  
17 are self-consistent, as shown in table 2. By substitution of values for  $G$  and  $\nu$  close to the  
18 measured values, the Lamé equations gave values for  $E$  close to those measured for the stored  
19 TMM. We conclude that the compressibility of the gels is a reflection of their complex  
20 polysaccharide structure containing numerous voids capable of deformation<sup>2</sup>. For the fresh agar  
21 gel, the three methods used in this study to measure Young's modulus gave small but significant  
22 differences. As shown in table 2, the LDS values were significantly lower than those obtained  
23 from the TM and Instron measurements ( $p = 0.004$  and  $0.02$  ( $n = 4$ ) respectively, Student's t-test)

1 whilst the TM and Instron results were in close agreement. When comparing the values obtained  
2 by the three methods for the stored specimens, no differences were found ( $n = 4$ ). For the shear  
3 modulus, the results from the LDS and Instron measurements were not significantly different in  
4 both the fresh and stored specimens. Given the good agreement between the three methods  
5 found in the stored specimens and the fact that the LDS measurements were performed up to 2  
6 hours before the TM and Instron experiments, we believe that the disparity in the fresh material  
7 is due to rapid changes in the properties of the gel in the period shortly after it is removed from  
8 the mould and needs further investigation. It is worth noting that under the quasi-static  
9 conditions used in these measurements, the relationship between stress and strain was linear  
10 from strains of zero up to 1%, with Pearson correlation coefficients ( $r^2$ ) typically  $> 0.998$  (Data  
11 not shown).

12  
13 Indentation tests<sup>28</sup> have shown that the Young's modulus for 3% agar was  $\sim 52$  kPa. Low and  
14 high viscosity agar gels have been measured elsewhere using an Instron tester<sup>26</sup>; the low  
15 viscosity gels had a compression modulus of 254 kPa at a concentration of 2.5%, whereas the  
16 high measured 516 kPa at a concentration of 3%. It is apparent that there is a range of measured  
17 values for this variable. Our results also appear consistent with data measured using HFVS<sup>21</sup>. In  
18 that study, the measured storage modulus,  $G'$ , for a 1.5% agar gel ranged between 200 - 300 kPa  
19 over the frequency range, 10 - 1000 Hz. Here also, in our reported results, the storage moduli  
20 were dispersive, which indicates viscosity. It is emphasised here that care should be taken to  
21 ensure a consistent gel manufacture process and with careful control of the manufacturing  
22 temperatures and heating rates we have found little variability in the properties of different gel  
23 batches.

1  
2  
3  
4  
5  
6  
7  
8  
9  
10  
11  
12  
13  
14  
15  
16  
17  
18  
19  
20  
21  
22  
23

In both creep experiments, the TMM became stiffer once it had been stored in water and it has been shown that this stored TMM has similar values for these elastic moduli as human muscle<sup>13</sup>. Neither the compressional nor shear creep curves appear to be reaching an asymptote, which implies that the TMM is a viscoelastic fluid. Also, neither set of curves returns to its initial displacement, which implies that the TMM is viscous. These contradictory observations confirm the complex structure and properties of these agar gels and we emphasise the need for carefully specifying the conditions under which measurements are made.

For the oscillations, it can be seen that the initial displacement on loading is approximately 50 % larger for the compressional experiment than for the shear set up, an observation in keeping with the measured quasi-static Young's and shear moduli. We note that the initial loaded deformation of around 0.3 mm corresponds to normal and shear strains of less than 1% and we therefore assume that the elastic response, under these conditions too, is linear. In both experiments, it is again apparent that the stored TMM is stiffer than the fresh. We observed little difference between the fresh and stored specimens in the number of oscillations both in the compressional, (~ 6-7), and shear, (~ 18-20), experiments, nor in their respective frequencies which, as they are free oscillations, presumably reflect a characteristic resonance mode. The amplitude of the free oscillations exhibits an exponential decay. These data have been used as input to a one dimensional viscoelastic model of wave propagation in viscoelastic media<sup>3</sup>. The agreement between the measured and computed displacement/time data was excellent and allowed us to obtain estimates of the dynamic Young's and shear moduli together with their corresponding relaxation times.

1  
2 As mentioned above, we have treated the elastic properties of the material under investigation as  
3 linear. Although the elastic response of soft tissues is non-linear under the large strains  
4 associated with the propagation of the arterial pulse wave and the movement of the heart itself,  
5 the displacement waves caused by the stenosis are very weak and such that, even in a soft  
6 biomaterial, are unlikely to cause geometric nonlinearities and hence there seems no need for  
7 finite strain measures. It is therefore reasonable to assume the existence of linear elastic  
8 constants such as Young's modulus and Poisson's ratio for the instantaneous elastic response of  
9 the viscoelastic material. The question of whether or not there is constitutive nonlinearity arising  
10 from the time constants is rather more delicate. Our hypothesis here, by operating in this fairly  
11 narrow range of dominant frequencies due to acoustic signature of the stenosis, is that there is no  
12 such nonlinearity. This will make our computational model simpler and help to make our  
13 anticipated diagnostic technology more practical. The inclusion of nonlinear effects can be  
14 considered later, if they are needed, and these will be issues for future research.

15

## 16 **Acoustic Properties**

17 Although there was a statistically significant correlation between attenuation and frequency,  
18 where the Pearson correlation coefficient for the 60 mm thickness was 0.65 and the p-value,  $p <$   
19 0.001 ( $n = 6$ ), strong, regular fluctuations of attenuation with frequency were observed with the  
20 maxima occurring at around 500, 900, 1300 and 1700 Hz, i.e. at approximately 400 Hz intervals,  
21 as seen in figure 7. These fluctuations appear for all three specimen thicknesses but are more  
22 pronounced in the thinner specimens. We speculate that they are due to interference from  
23 internal reflections within the block. Strong reflections might also be expected to cause

1 fluctuation in the apparent (i.e. measured) wave speed but, as figure 8 shows, these are less  
2 prominent. The possibility of reflections will be investigated in another study in which the  
3 impulse response within a cylindrical gel specimen will be analysed. As with the other measures  
4 of elasticity reported here the strains induced are small, in this case  $< 1\mu\text{m}$ , and we again assume  
5 that the elastic response is linear.

6  
7 The value for attenuation at 300 Hz for the 60 mm thickness, as derived from the data in figure 7,  
8 is approximately  $320 \pm 30 \text{ dB m}^{-1}$ , (SEM,  $n = 6$ ). This is equivalent to a value of  $37 \text{ Np m}^{-1}$ .  
9 Other studies have limited their measurement frequency range up to 200 Hz<sup>18,26</sup>. In one study,  
10 an unexpected decrease in attenuation was seen in the frequency range 100 - 200 Hz<sup>22</sup>, whereas  
11 elsewhere a rise was seen with a coefficient of approximately  $25 \text{ Np m}^{-1}$  per 100 Hz<sup>17</sup>. It can be  
12 seen that, given the disparate experimental conditions in the various reports, our data agree  
13 reasonably well with previously published values and closely with the results of  $40 \text{ Np m}^{-1}$   
14 obtained at 300 Hz<sup>22</sup>.

15  
16 Shear wave velocity has been measured in 3 % agar / 3 % gelatin gel at approximately  $2.1 \text{ ms}^{-1}$   
17 over the frequency range of 50 - 200 Hz<sup>17</sup>, where it was also found to be frequency  
18 independent. Liver tissue was measured using shear wave spectroscopy and found to have a  
19 shear wave velocity of  $1.5 - 3 \text{ ms}^{-1}$  for the frequency range 75 – 500 Hz<sup>13</sup>. Our results measured  
20 at 300 Hz, i.e. close to the frequencies in the studies mentioned above, correspond well to that  
21 published with a velocity at approximately  $3 \text{ ms}^{-1}$ . We observed that the phase velocity increases  
22 with frequency and that the rate of increase is highest at low frequencies. This observation may  
23 fit with a Maxwellian rheological model but conflicts with previous studies that suggest the

1 velocity remains constant with frequency over the range 100-500 Hz<sup>9,10,11,22</sup>. However, the  
2 variation of velocity with frequency seen here matches well with values obtained from agar  
3 plates measured using shear wave imaging<sup>12</sup>. Measurements at higher frequencies, beyond  
4 those of relevance to this study, would be needed to ascertain whether the velocity is tending  
5 towards an asymptotic value.

6

7 The acoustic properties of the TMM change with frequency. The attenuation increases linearly  
8 at a rate of 1.9 dB cm<sup>-1</sup> kHz<sup>-1</sup>. The phase speed also increases with frequency and although the  
9 rate of change decreases with frequency. It shows no tendency to reach an asymptotic value.

10

11 The experiments described here have provided baseline values of the acoustic and elastic  
12 properties of tissue mimicking materials from which we are currently manufacturing soft tissue  
13 phantoms of the chest and in which we are measuring the propagation of mechanically generated  
14 and flow induced shear waves. Data from these experiments, the next step towards our longer  
15 term aim of producing a diagnostic instrument, will be reported in due course.

16

### 17 **Conflict of Interest**

18 No benefits in any form have been or will be received from a commercial party related directly  
19 or indirectly to the subject of this manuscript.

20

### 21 **7. Acknowledgements**

22 This work is supported by the Engineering and Physical Sciences Research Council (EPSRC)  
23 [EP/H011072/1 and EP/H011285/1].

24

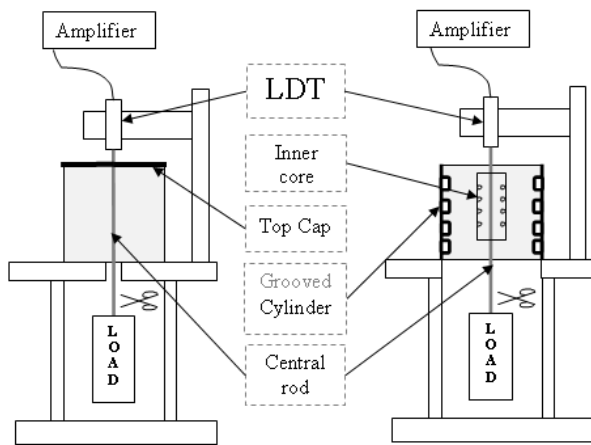
## 1 8. References

- 2 1. AIUM. Methods for specifying acoustic properties of tissue mimicking phantoms and objects,  
3 Stage I. Laurel, MD, American Institute of Ultrasound in Medicine Technical Standards  
4 Committee. 1995.
- 5 2. Arnott S, Fulmer A, Scott WE, Dea IC, Moorhouse R, Rees DA. The agarose double helix and  
6 its function in agarose gel structure. *J Mol Biol.* 90(2): 269-284, 1974.
- 7 3. Banks HT, Hu S, Kenz ZR, Kruse C, Shaw S, Whiteman JR, Brewin MP, Greenwald SE,  
8 Birch MJ. Material parameter estimation and hypothesis testing on a 1D viscoelastic stenosis  
9 model: Methodology. *J Inverse and Ill-posed Problems.* 21(1): 25-57, 2013.
- 10 4. Banks HT, Hu S, Kenz ZR, Kruse C, Shaw S, Whiteman JR, Brewin MP, Greenwald SE,  
11 Birch MJ. Model validation for a noninvasive arterial stenosis detection problem mathematical  
12 biosciences and engineering. *IJNME.* 11(3): 427-448, 2014.
- 13 5. Brewin MP, Pike LC, Rowland DE, Birch MJ. The acoustic properties, centered on 20 MHz,  
14 of an agar-based tissue-mimicking material and its temperature, frequency and age dependence.  
15 *Ultrasound Med Biol.* 34(8): 1292-1306, 2008.
- 16 6. Brewin M.P, Srodon PD, Greenwald SE, Birch MJ. Carotid atherosclerotic plaque  
17 characterisation by measurement of ultrasound sound speed in vitro at high frequency, 20 MHz.  
18 *Ultrasonics.* 54(2): 428-441, 2014.
- 19 7. Browne JE, Ramnarine KV, Watson AJ, Hoskins PR. Assessment of the acoustic properties of  
20 common tissue mimicking test phantoms. *Ultrasound Med Biol.* 29(7): 1053-1060, 2003.
- 21 8. Burlew MM, Madsen EL, Zagzebski JA, Banjavic RA, Sum SW. A new ultrasound tissue-  
22 equivalent material. *Radiology.* 134(2): 517-520, 1980.

- 1 9. Catheline S, Wu F, Fink M. A solution to diffraction biases in sonoelasticity: The acoustic  
2 impulse technique. *J Acoust Soc Am*. 105(5): 2941-2950, 1999.
- 3 10. Catheline S, Sandrin L, Gennisson J-L, Tanter M, Fink M. Ultrasound-based noninvasive  
4 shear elasticity probe for soft tissues. *IEEE Ultrasonics Symposium*. 2: 1799-1801, 2000.
- 5 11. Catheline S, Gennisson J-L, Delon G, Fink M, Sinkus R, Abouelkaram S, Culioli J.  
6 Measurement of viscoelastic properties of homogeneous soft solid using transient elastography:  
7 An inverse problem approach. *J Acoust Soc Am*. 116(6): 3734-3741, 2004.
- 8 12. Couade M, Pernot M, Prada C, Messas E, Emmerich J, Bruneval P, Criton A, Fink M, Tanter  
9 M. Quantitative assessment of arterial wall biomechanical properties using shear wave imaging.  
10 *Ultrasound Med Biol*. 2010; 36(10): 1662-76.
- 11 13. Deffieux T, Montaldo G, Fink M. Shear wave spectroscopy for in vivo quantification of  
12 human soft tissues visco-elasticity. *IEEE Trans Med Imaging*. 28(3): 313-322, 2009.
- 13 14. Dineley J, Meagher S, Poepping TL, McDicken WN, Hoskins PR. Design and  
14 characterisation of a wall motion phantom. *Ultrasound Med Biol*. 32(9): 1349-1357, 2006.
- 15 15. Feng K and Shi Z-C. *Mathematical theory of elastic structures*. New York: Springer, 1981.
- 16 16. Fromageau J, Brusseau E, Vray D. Characterization of PVA cryogel for intravascular  
17 ultrasound elasticity imaging. *IEEE-UFFC*. 50(10): 1318-1323, 2003.
- 18 17. Gennisson J-L and Cloutier G. Sol-gel transition in agar-gelatin mixtures studied with  
19 transient elastography. *IEEE-UFFC*. 53(4): 716 –723, 2006.
- 20 18. Glagov S. Intimal hyperplasia, vascular modeling, and the restenosis problem. *Circulation*.  
21 89(6): 2888-2891, 1994.

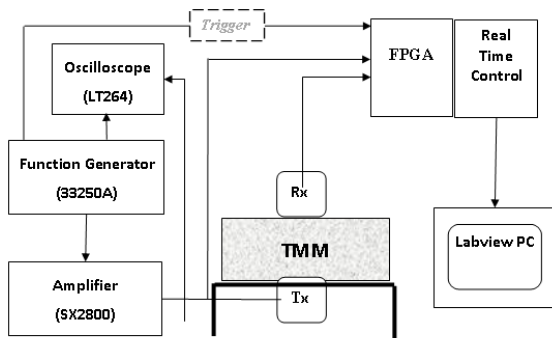
- 1 19. Glozman T and Azhari H. A method for characterization of tissue elastic properties  
2 combining ultrasonic computed tomography with elastography. *J Ultrasound Med.* 29(3): 387-  
3 398, 2010.
- 4 20. Gray DE. *American Institute of Physics Handbook*. 3rd ed. New York: McGraw Hill. 1973.
- 5 21. Hadj Henni A, Schmitt C, Tremblay MÉ, Hamdine M, Heuzey MC, Carreau P, Cloutier G.  
6 Hyper-frequency viscoelastic spectroscopy of biomaterials. *J Mech Behav Biomed Mater.* 4(7):  
7 1115-1122, 2011.
- 8 22. Klinkosz T, Lewa CJ, Paczkowski J. Propagation velocity and attenuation of a shear wave  
9 pulse measured by ultrasound detection in agarose and polyacrylamide gels. *Ultrasound Med*  
10 *Biol.* 34(2): 265-275, 2008.
- 11 23. Madsen EL, Zagzebski JA, Banjavic RA, Jutila RE. Tissue mimicking materials for  
12 ultrasound phantoms. *Med Phys.* 5(5): 391–394, 1978.
- 13 24. Madsen EL, Zagzebski JA, Frank GR. Oil-in-gelatin dispersions for use as ultrasonically  
14 tissue-mimicking materials. *Ultrasound Med Biol.* 8(3): 277–287, 1982.
- 15 25. Madsen EL, Hobson MA, Shi H, Varghese T, Frank GR. Tissue-mimicking agar/gelatin  
16 materials for use in heterogeneous elastography phantoms. *Phys Med Biol.* 50(23): 5597-5618,  
17 2005.
- 18 26. Normand V, Lootens DL, Amici E, Plucknett KP, Aymard P. New insight into agarose gel  
19 mechanical properties. *Biomacromolecules.* 1(4): 730-738, 2000.
- 20 27. Poepping TL, Nikolov HN, Thorne ML, Holdsworth DW. A thin-walled carotid vessel  
21 phantom for Doppler ultrasound flow studies. *Ultrasound Med Biol.* 30(8): 1067-1078, 2004.
- 22 28. Ross KA. and Scanlon MG. Analysis of the elastic modulus of agar gel by indentation. *J*  
23 *Texture Studies.* 30(1): 17-27, 1999.

- 1 29. Semmlow JL and Rahalkar K. Acoustic detection of coronary artery disease. *Ann Rev*
- 2 *Biomed Eng.* 9: 449-469, 2007.
- 3 30. Thrush AJ, Brewin MP, Birch MJ. Assessment of tissue Doppler imaging measurements of
- 4 arterial wall motion using a tissue mimicking test rig. *Ultrasound Med Biol.* 34(3): 446-53, 2008.
- 5



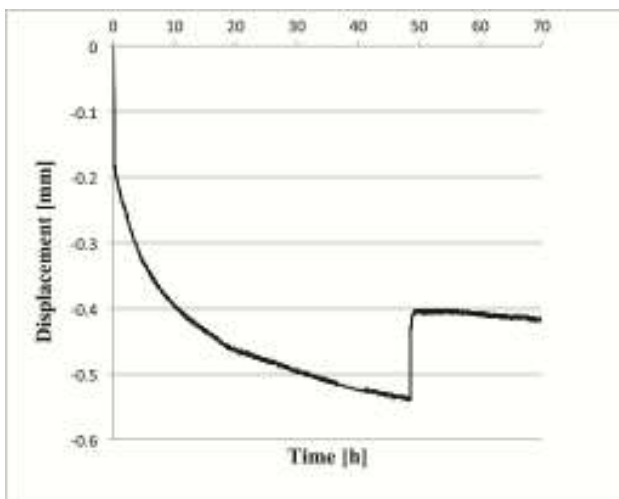
1

2 Figure 1 (Brewin)



3

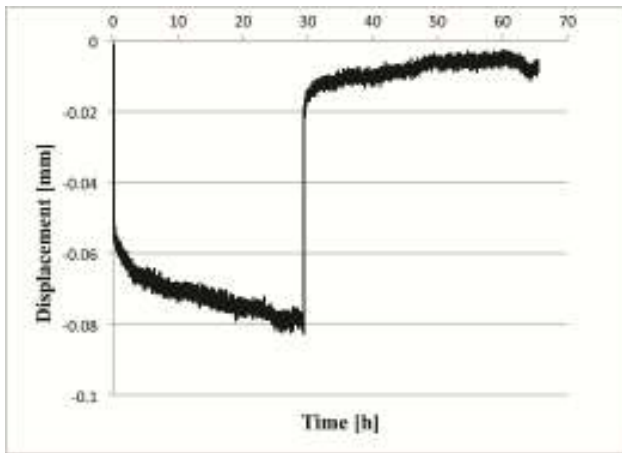
4 Figure 2 (Brewin)



5

6 Figure 3 (Brewin)

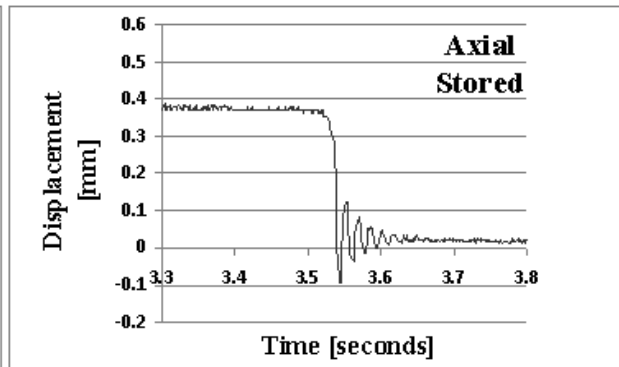
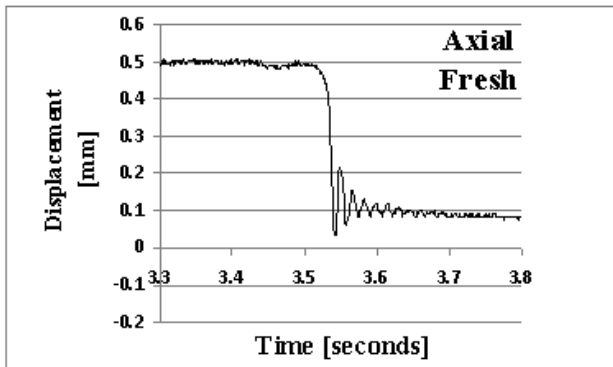
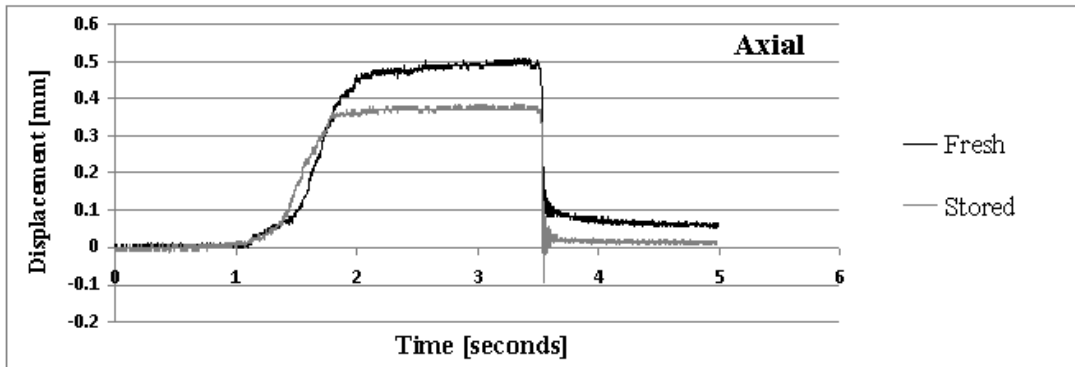
7



1

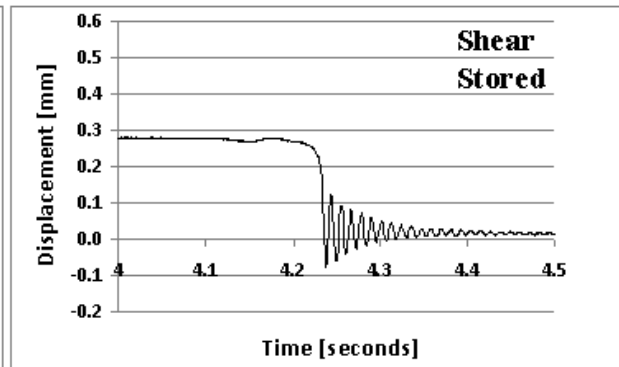
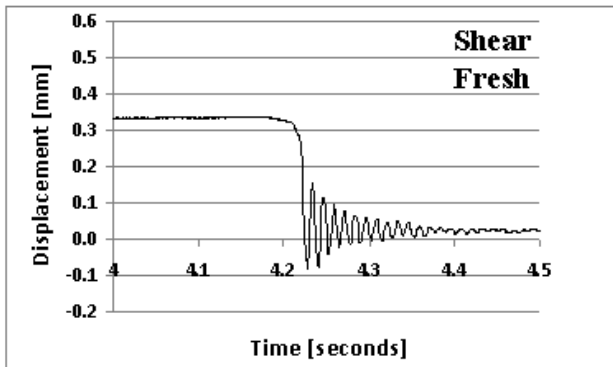
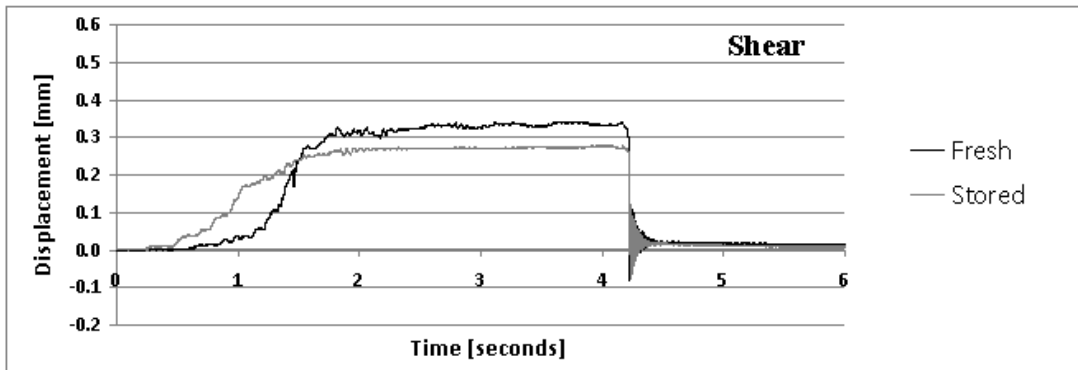
2 Figure 4 (Brewin)

3



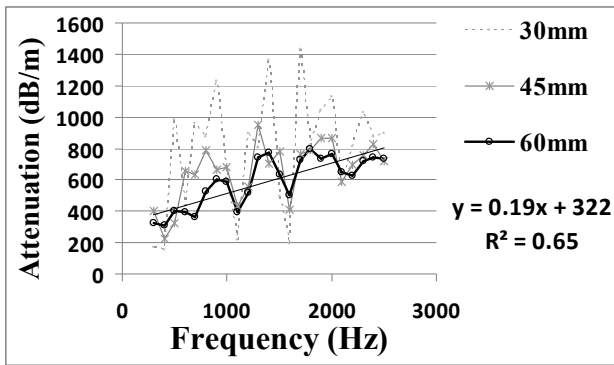
1

2 Figure 5 (Brewin)



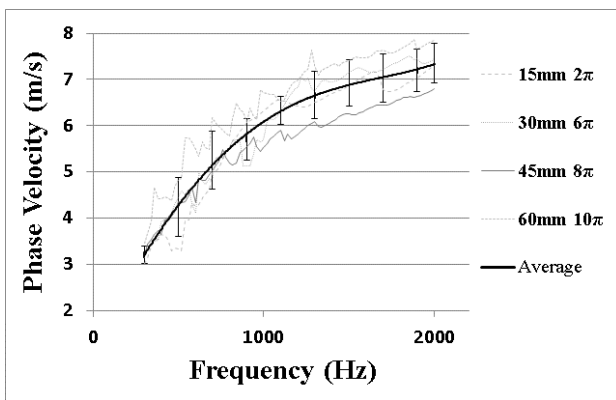
3

4 Figure 6 (Brewin)



1

2 Figure 7 (Brewin)



3

4 Figure 8 (Brewin)

5

1

<b>Elastic Modulus</b>	<b>Experiment</b>	<b>Fresh</b>	<b>Stored</b>
<b>Young's, E (kPa)</b>	TM (n=7)	<b>122 ± 8</b>	<b>155 ± 22</b>
	LDS (n=4)	<b>110 ± 3</b>	<b>150 ± 6</b>
	INSTRON (n=4)	<b>123 ± 6</b>	<b>157 ± 8</b>
<b>Shear, G (kPa)</b>	LDS (n=4)	<b>52 ± 3</b>	<b>54 ± 2</b>
	INSTRON (n=4)	<b>52 ± 3</b>	<b>56 ± 4</b>
<b>Poisson's Ratio, <math>\nu</math></b>	TM (n=7)	<b>0.37 ± 0.07</b>	<b>0.44 ± 0.08</b>

2

3 Table 1: Elastic moduli of both fresh and stored TMM, measured using the travelling microscope  
4 (TM), the linear displacement transducer (LDS) and the Instron. The values are the mean of n  
5 determinations  $\pm$  1 SD.

6

1

Elastic Modulus	Experiment	Fresh		Stored	
		Measured	Lamé	Measured	Lamé
Young's, E (kPa)	TM (n=7)	122 ± 8	148	155 ± 22	158
	LDS (n=4)	110 ± 3		150 ± 6	
	INSTRON (n=4)	123 ± 6		157 ± 8	
Shear, G (kPa)	LDS (n=4)	52 ± 3	52	54 ± 2	55
	INSTRON (n=4)	52 ± 3		56 ± 4	
Poisson's Ratio, $\nu$	TM (n=7)	0.37 ± 0.07	0.37	0.44 ± 0.08	0.44

2

3 Table 2: Calculation of Young's modulus from the measured values of shear modulus and  
4 Poisson's ratio using the Lamé expression. This enables comparison of measured values with  
5 predicted values. The three experiments are TM – Travelling microscope, LDS – Incremental  
6 Load & Instron. The values are the mean of n determinations ± 1 SD.

7

1 **Figure Captions**

2

3 Figure 1: The compressional, left, and shear, right, set up for the measurement of moduli, creep  
4 and free oscillations. The load is applied to the Perspex top cap in compressional mode and to  
5 the inner core for the shear measurements. The scissors represent the sudden release of the load  
6 in the free oscillation experiment as described in the method.

7

8 Figure 2: Block diagram for the wave propagation measurements. Tx and Rx signify the transmit  
9 and receive accelerometers. TMM is the block of tissue mimicking material resting on the  
10 Perspex frame (bold line). The FPGA is the field-programmable gate array module.

11

12 Figure 3: A typical time-displacement curve showing the axial creep of the TMM cylinder. The  
13 48 g load was applied at time zero and removed after 50 hours.

14

15 Figure 4: A typical time-displacement curve showing the shear creep of the TMM cylinder. The  
16 48 g load was applied time zero and removed after 30 hours.

17

18 Figure 5: The free compressional oscillations induced in the compressional experiment for 264 g  
19 load. The top panel shows both time-displacement plots in their entirety. The bottom two panels  
20 show the magnified section of the free oscillations for fresh and stored TMM respectively.

21

1 Figure 6: The free shear oscillations induced in the shear experiment for 264 g load. The top  
2 panel shows both time-displacement plots in their entirety. The bottom two panels show the  
3 magnified section of the free oscillations for fresh and stored TMM respectively.

4  
5 Figure 7: Frequency dependence of attenuation of three different thicknesses (30 mm, 45 mm  
6 and 60 mm) of the agar-based TMM, normalised to a 15mm thick sample.

7  
8 Figure 8: Frequency dependence of phase velocity over the range, 300 – 2000 Hz. Each  
9 thickness has its associated  $2n\pi$  phase addition as detailed in the legend. Error bars show  $\pm 1$   
10 SD.